Molecular BioSystems

PAPER

Cite this: *Mol. BioSyst.*, 2015, 11, 2925

Intrinsically disordered amphiphilic peptides as potential targets in drug delivery vehicles

Marian Vincenzi,†[abc] Antonella Accardo,†[ab] Susan Costantini,[d] Stefania Scala,[e] Luigi Portella,[e] Annamaria Trotta,[e] Luisa Ronga,[c] Jean Guillon,[c] Marilisa Leone,[b] Giovanni Colonna,[f] Filomena Rossi[a] and Diego Tesauro*[ab]

Received 27th May 2015,
Accepted 1st August 2015

DOI: 10.1039/c5mb00358j

www.rsc.org/molecularbiosystems

Intrinsically disordered proteins/peptides play a crucial role in many physiological and pathological events and may assume a precise conformation upon binding to a specific target. Recently, we have described the conformational and functional properties of two linear ester peptides provided with the following sequences: Y-G-E-C-P-C-K-OAllyl (PepK) and Y-G-E-C-P-C-E-OAllyl (PepE). Both peptides are characterized by the presence of the "CPC" motif together with a few amino acids able to promote disorder. The CPC sequence is a binding motif for the CXCR4 receptor that represents a well-known target for cancer therapies. In this paper, we report on synthetic amphiphilic peptides that consist of lipophilic derivatives of PepE and PepK bearing two stearic alkyl chains and/or an ethoxylic spacer. These peptide amphiphiles form stable supramolecular aggregates; they present conformational features that are typical of intrinsically disordered molecules as shown by CD spectroscopy. Solution fluorescence and DLS studies have been performed to evaluate Critical Micellar Concentrations and the dimension of supramolecular aggregates. Moreover, preliminary *in vitro* cell-based assays have been conducted to investigate the molecular recognition processes involving the CXCR4 receptor. In the end, the results obtained have been compared with the previous data generated by the corresponding non-amphiphilic peptides (PepE and PepK).

1. Introduction

Peptides may carry out a broad range of biological functions while acting as growth factors, neurotransmitters, and hormones.[1–5] The regulatory role that they may play in physiological tasks has pushed pharmacologists to exploit peptides as therapeutic[6,7] or diagnostic tools.[8,9] Peptide drugs can offer many advantages: they have specific features but they have a broad spectrum of activity; they have less side effects than organic molecules; they allow an infinite array of sequences which could be designed in order to regulate physiological processes.[10] Peptides can act as agonists or antagonists of biomolecular processes by interacting with cell surface receptor systems that show over-expression in several neoplastic and non-neoplastic cells.[11] As the CXCR4 receptor is overexpressed in several human cancers, it is considered one of the most relevant targets in drug discovery. The blockade of the CXCR4–CXCL12 interaction has been extensively investigated as a potential research path for new cancer therapies.[12] Recently, we have designed and synthesized a CPC motif containing peptides by using the N-terminal region of CXCL12 as a template.[13]

Afterwards, we generated two novel linear ester peptides containing the following sequences: Y-G-E-C-P-C-K-OAllyl (PepK) and Y-G-E-C-P-C-E-OAllyl (PepE). Both these peptides are characterized by the presence of the same CPC motif together with a few amino acids able to foster disorder.[14] For PepE and PepK, NMR and circular dichroism (CD) spectra have revealed the lack of well-defined secondary structure elements, thus confirming their high conformational flexibility. Moreover, molecular dynamics (MD) simulations have pointed out that PepE and PepK could dynamically explore conformational ensembles, thanks to the absence of a regular secondary structure. We have also preliminary tested the biological properties of these peptides: they have targeted CXCR4 and they have modulated the adenylate cyclase

[a] *Department of Pharmacy and CIRPeB University of Naples "Federico II", Via Mezzocannone 16, I-80134 Naples, Italy. E-mail: diego.tesauro@unina.it; Fax: +39 0812534574; Tel: +39 0812536643*
[b] *Istituto di Biostrutture e Bioimmagini – CNR, Via Mezzocannone 16, I-80134, Naples, Italy*
[c] *UFR des Sciences Pharmaceutiques - Collège Sciences de la Santé, INSERM U869, Laboratoire ARNA, Université de Bordeaux, 146 rue Léo Saignat, 33076 Bordeaux cedex, France*
[d] *CROM, Istituto Nazionale Tumori "Fondazione G. Pascale", IRCCS, I-80131 Napoli, Italy*
[e] *Molecular Imunology and Immuneregulation, Istituto Nazionale Tumori "Fondazione G. Pascale", IRCCS, I-80131 Napoli, Italy*
[f] *Servizio di Informatica Medica, Azienda Ospedaliera Universitaria, Seconda Università di Napoli, I-80138 Napoli, Italy*
† These authors contributed equally to this work.

production with remarkable performances, better than the ones obtained so far by AMD3100 *i.e.*, a known CXCR4 antagonist.

The application of an intrinsically disordered peptide as a biosensor (or even in molecular recognition) could rely on its own capability to control the transition between different structural states.[15] One opportunity to induce conformational peptide rearrangement could be achieved by modifying the bioactive peptide sequence with a hydrophobic moiety. This modification led to the design of peptide amphiphiles (PAs), a class of emergent molecules, that, by combining the structural features of amphiphilic surfactants with the functions of bioactive peptides,[16–18] are useful for biotechnological applications in drug delivery of pharmacological molecules.[19–21] Furthermore, PAs are able to self-assemble into a wide variety of nanostructures, such as spherical entities with a cylindrical geometry or rod like micelles, monolayers, bilayers, vesicles and nanofibers. Supramolecular aggregation of PAs is driven by the presence of both hydrophilic and hydrophobic moieties. In detail, the hydrophilic moiety is composed of a bioactive peptide sequence enriched with hydrophilic amino acids. In addition, the sequence can be improved by an ethoxylic linker. The hydrophobic moiety is made of hydrocarbon groups such as one or two long alkyl chains containing more than ten carbon atoms.

Taking into account these elements, we have designed lipophilic derivatives of PepE and PepK bearing two stearic alkyl chains and/or an ethoxylic spacer. The structural characterization of self-assembled PAs in aqueous solution was assessed by fluorescence spectroscopy and Dynamic Light Scattering (DLS), while the conformational preferences were evaluated by CD. To test the binding properties and the biological behaviour of peptides, biological assays were also carried out in cells overexpressing the CXCR4 receptor. Finally, the structural features revealed by this study were compared with the ones previously found for disordered linear peptides.

2. Materials and Methods

2.1. Reagents

All N^{α}-Fmoc-amino acid derivatives, 2-chlorotrityl chloride resin pre-loaded with Fmoc-Glu-OAllyl and Fmoc-Lys-OAllyl and coupling reagents were purchased from Calbiochem-Novabiochem (Laufelfingen, Switzerland), Iris Biotech GMBH (Marktredwitz, Germany) or from Inbios (Napoli, Italy). Fmoc-21-amino-4,7,10,13,16,19-hexaoxaheneicosanoic acid (Fmoc-Ahoh-OH) was purchased from Neosystem (Strasbourg, France). *N*,*N*-Dioctadecylsuccinamic acid was synthesized according to the published methods.[22] All other chemicals were commercially available by Sigma-Aldrich (Milano, Italy) and were used as received unless otherwise stated.

Preparative RP-HPLC was carried out on a LC8 Shimadzu HPLC system (Shimadzu Corporation, Kyoto, Japan) equipped with a UV lambda-Max Model 481 detector using a Phenomenex (Torrance, CA) C4 (300 Å, 250 × 21.20 mm, 5 μ) column. Elution solvents are H_2O/0.1% TFA (A) and CH_3CN/0.1% TFA (B), from 20% to 95% over 20 minutes at 20 mL min^{-1} flow rate. The purity and identity of the products were assessed by analytical LC–MS analyses by using Finnigan Surveyor MSQ single quadrupole electrospray ionization (Finnigan/Thermo Electron Corporation San Jose, CA), column C4-Phenomenex eluted with an H_2O/0.1% TFA (A) and CH_3CN/0.1% TFA (B) from 20% to 95% over 20 minutes at 0.8 mL min^{-1} flow rate.

2.2. Amphiphilic peptide synthesis

All amphiphilic peptides were synthesized following a solid phase peptide standard protocol using Fmoc chemistry on 2-chlorotrityl chloride resin pre-loaded (0.24 scale mmol) with the side chain of α Fmoc-Lys-OAllyl and α Fmoc-Glu-OAllyl, respectively. The sequence H-YGECPC was built on both resins. In particular the resins were allowed to swell in dichloromethane (DCM) and Fmoc-deprotection steps were performed by treating the resin for 30 min in a dimethylformamide (DMF)/Piperidine (Pip) (80/20, v/v) solution.

For coupling steps the resin was suspended in DMF containing three equivalents of the Fmoc-protected amino acid, O-benzotriazole-tetramethyl-uronium-hexafluoro-phosphate (HBTU), and diisopropylethylamine (DIEA) (6 eq.), and the reaction mixture was shaken for 2 h at room temperature. The Fmoc ethoxylic spacer and lipophilic *N*,*N*-dioctadecylsuccinic acid were coupled, as previously described.[23]

Peptides were cleaved by soaking the resin in TFA/H_2O/triisopropylsilane (TIS) (3.0 mL, 95/2.5/2.5, v/v/v) for 3 h. Cleavage mixtures were filtered from the resin and crude products were precipitated by adding cold water, centrifuged, and decanted. The resulting white solids were dissolved in a water and acetonitrile 4 : 1 v : v (10 mL) mixture and freeze-dried to obtain a white powder that was analyzed for purity and purified by preparative RP-HPLC. Purified peptides were characterized by LC-ESI-MS. Mass values found: 1443 a.m.u. [$(C18)_2$-PepE]; 1442 a.m.u. [$(C18)_2$-PepK];1776 a.m.u. [$(C18)_2$-L-PepK]; 1777 a.m.u. [$(C18)_2$-L-PepE].

2.3. Preparation of aggregate solutions

Samples were prepared by dissolving the lyophilized PAs in aqueous solutions. In detail, $(C18)_2$-PepK and $(C18)_2$-L-PepK were dissolved in 10 mM TRIS buffer at pH 8.0, whereas $(C18)_2$-PepE and $(C18)_2$-L-PepE in 10 mM phosphate buffer (PBS) at pH 7.4. The pH-meter was calibrated with three standards at pH 4.00, pH 7.00 and pH 10.00. In most cases the samples to be measured were prepared from stock solutions. The concentrations of all solutions were determined by UV-Vis absorbance measurements carried out on a Thermo Fisher Scientific Inc (Wilmington, Delaware USA) Nanodrop 2000c spectrophotometer equipped with a 1.0 cm quartz cuvette (Hellma) using a molar absorptivity (ε) of 1390 M^{-1} cm^{-1} at λ = 275 nm, which corresponds to the wavelength of the tyrosine residue.

2.4. Fluorescence measurements

Values of critical micellar concentration (CMC) of peptide amphiphiles were obtained by fluorescence measurements. Fluorescence spectra were recorded at room temperature on a

Jasco Model FP-750 spectrofluorophotometer (Jasco Int. Co. Ltd, Tokio, Japan) in a 1.0 cm path length quartz cell. Equal excitation and emission bandwidths were used throughout the experiments, with a recording speed of 125 nm min^{-1} and automatic selection of the time constant. CMC values were measured by using 8-anilino-1-naphthalene sulfonic acid ammonium salt (ANS) as the fluorescent probe.[24] Small aliquots of peptide aqueous solution were added to a fixed volume (1.00 mL) of 2.0×10^{-5} M ANS fluorophore directly in the quartz cell. CMC values were determined by linear least-squares fitting of the fluorescence emission at 480 nm, upon excitation at 350 nm *versus* the amphiphile concentration. Fluorescence emission spectra of the tyrosine residue in the PAs were recorded at 5×10^{-5} M concentration and 25 °C exciting the peptide solution at 275 nm.

2.5. Dynamic light scattering characterization

Dynamic light scattering (DLS) measurements were carried out using a Zetasizer Nano ZS (Malvern Instruments, Westborough, MA) that employs a 173° backscatter detector. Other instrumental settings are measurement position (mm): 4.65; attenuator: 8; temperature 25 °C; cell: disposable sizing cuvette. DLS samples were prepared at a final concentration of 2.0 10^{-4} M and centrifuged at room temperature at 13 000 rpm for 5 min.

2.6. CD measurements

Far-UV CD spectra were recorded from 260 to 190 nm on a Jasco J-810 spectropolarimeter equipped with a NesLab RTE111 thermal controller unit using a 1 mm quartz cell at 25 °C. CD spectroscopy of alkylated derivatives of PepE and PepK was carried out at 2.0×10^{-4} M concentration in 2.0 mM phosphate buffer and 10 mM TRIS, respectively. Other experimental settings were: scan speed, 10 nm min^{-1}; sensitivity, 50 mdeg; time constant, 16 s; bandwidth, 1 nm. Each spectrum was obtained averaging three scans, and by subtracting contributions from other species in solution and converting the signal to mean residue ellipticity in units of deg cm^2 $dmol^{-1}$ res^{-1}.

2.7. Biological test

The binding between CXCR4 and the four peptides was evaluated as previously described.[25] Briefly 2.5×10^5 CCRF–CEM cells were pre-incubated with 10 μM antagonist peptides in binding buffer (PBS 1× plus 0.2% BSA and 0.1% NaN_3) for 1h at 37 °C, 5% CO_2 and then labeled for 45 minutes with an anti-CXCR4 PE-antibody (FAB170P, clone 12G5, R&D Systems, Minneapolis, MN, USA). Cells were washed in PBS and analyzed using an FACS Canto II cytofluorimeter (Becton Dickinson Immunocytometry Systems, Mountain View, CA, USA). CCRF-CEM cell migration was assayed in 24-well Transwell chambers (Corning Inc., Corning, NY) using inserts with an 8 μm pore membrane. Membranes were pre-coated with collagen (human collagen type I/III) and fibronectin (20 mg mL^{-1} each). CCRF-CEM cells were placed in the upper chamber (1×10^5 cells per well) in RPMI containing 1% BSA (migration media). Cells were pre-incubated for 45 min with the CXCR4 antagonist and allowed to migrate toward 100 ng mL^{-1} CXCL12 in the lower chamber. After 16 h incubation, migrated cells were collected from the lower chamber and counted. The migration index was defined as the ratio between migrating cells in the experimental group and migrated cells in the control group.

We have conducted c-AMP–assay by using CCRF-CEM cells (1×10^6) that were incubated in the presence of four peptides or Plerixafor (known as AMD3100: a CXCR4 antagonist) that has provided proof of concept for inhibition of the CXCR4 pathway[26] at two different concentrations (1 and 10 μM) in combination with forskolin (F) (1 μM) for 20 min, followed by stimulation with CXCL12 (100 ng mL^{-1}) for 10 min. Controls include cells stimulated with CXCL12 and forskolin or forskolin alone in the absence of anti-CXCR4 inhibitors. Cells have been harvested and lysed with 0.1 M HCl and cAMP levels have been assayed by a direct competitive enzyme immunoassay (BioVision Incorporated) according to manufacture instructions.

3. Results and discussion

3.1. Design and synthesis

Recently we synthesized two linear intrinsically disordered peptides, PepK and PepE, based on the same sequence (YGECPC). This sequence was designed choosing amino acids with disorder propensity.[14] Subsequently, PepK and PepE were obtained by adding one charged residue at the C-terminus. In the case of PepK the charged residue was lysine, whilst PepE was provided with glutamic acid. The charged amino acids, namely Lys and Glu, were introduced in order to evaluate the influence of negative and positive charges on the aggregation of short sequence structures. Peptide amphiphiles, $(C18)_2$-PepK and $(C18)_2$-PepE, reported in Fig. 1 were obtained by conjugating two aliphatic chains of eighteen carbon atoms at the N-terminus of both sequences. Two other PA derivatives, indicated in Fig. 1 as $(C18)_2$-L-PepK and $(C18)_2$-L-PepE, were obtained by inserting the AhOh exoethylene linker between the peptide sequence and the hydrophobic double-tail. This linker, the same for both peptides, allows us to increase the hydrophilicity of PAs without modifying their final charge, in this way avoiding intra- and inter-electrostatic interactions. Indeed, the insertion of the

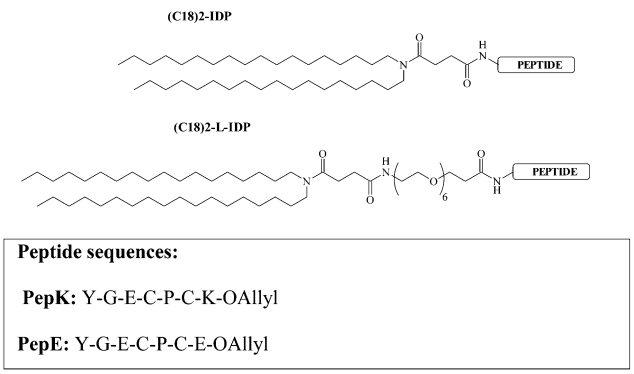

Fig. 1 Schematic representation of $(C18)_2$-PepK, $(C18)_2$-PepE and $(C18)_2$-L-PepK and $(C18)_2$-L-PepE. The peptide sequences are reported using the one-letter amino acid code.

linker leads to the distancing between the bioactive peptide and the hydrophobic shell of the aggregates. The relatively short length of this moiety was chosen in order to avoid possible formation of a hydrophilic pocket, able to hide the amino acid sequences. Finally, as is well-known from the literature,[27] the presence of PEG chains can increase the *in vivo* blood circulation of self-assembled PA aggregates. PAs were synthesized according to standard solid phase peptide synthesis protocols using 2-Cl-(Trt)-Cl preloaded resin as a polymeric support. The ethoxylic moiety and the two alkyl chains at the N-terminus of both peptide sequences were added as previously reported.[23] After RP-HPLC purification, the products were identified by ESI-MS spectrometry.

3.2. Aggregate preparation and structural characterization

Supramolecular aggregates of pure PA derivatives were obtained by dissolving the lipophilic derivatives in 10 mM phosphate buffer (pH 7.4) for PepE and in 10 mM TRIS buffer (pH 8.0) for PepK. The choice of buffers to be used for solubilizing monomers was imposed by their different propensities to aggregate. In fact, according to the pKa values of glutamic acid and lysine residues, all PAs have shown a net charge in a neutral or slightly basic water solution: negative in PepE and positive in PepK. Self-aggregation properties of the amphiphilic peptides were investigated by fluorescence spectroscopy and DLS.

Critical micellar concentration (CMC) values were estimated by fluorescence spectroscopy by using ANS as a fluorescent probe. The fluorescence intensity of ANS depends on the surrounding environment. The ANS fluorophore emits only in a hydrophobic environment such as the hydrophobic core of a micellar aggregate, whereas it does not emit in water solution. CMC values can be estimated according to the data provided by the graphical break-point, reported in Fig. 2. These data have been obtained by plotting the fluorescence intensity of ANS in the emission maximum at 470 nm, as a function of the PA derivative concentration. Table 1 displays CMC values: 7.0×10^{-6} mol kg^{-1} for $(C18)_2$-PepK and 1.9×10^{-5} mol kg^{-1} for $(C18)_2$-L-PepK. These values indicate that the introduction of the ethoxylic linker slightly affects the formation of aggregates capable of capturing the ANS, but they also confirm the high stability of both the resulting aggregates. Furthermore, these values comply with those previously found for peptide amphiphiles containing the same hydrophobic moiety.[28,29] Nonetheless, the CMC values of both the amphiphilic derivatives of PepE are higher than the corresponding ones for PepK. This behaviour indicates that PepE owns a lower propensity to aggregate if compared to PepK; this may depend on the different interaction of the charges with the buffer salts. Data obtained by the DLS for all compounds are summarized in Table 1: the hydrodynamic radii, R_H; the diffusion coefficients, D; and the polydispersity indices, PDI. Measurements were performed at $\theta = 173^\circ$ on self-assembled PAs at a concentration of 2×10^{-4} mol kg^{-1} in the previously reported buffer solution. All aggregate solutions show a monomodal distribution, which indicates the presence of just one population of aggregates. At infinite dilution, R_H values can be examined by using

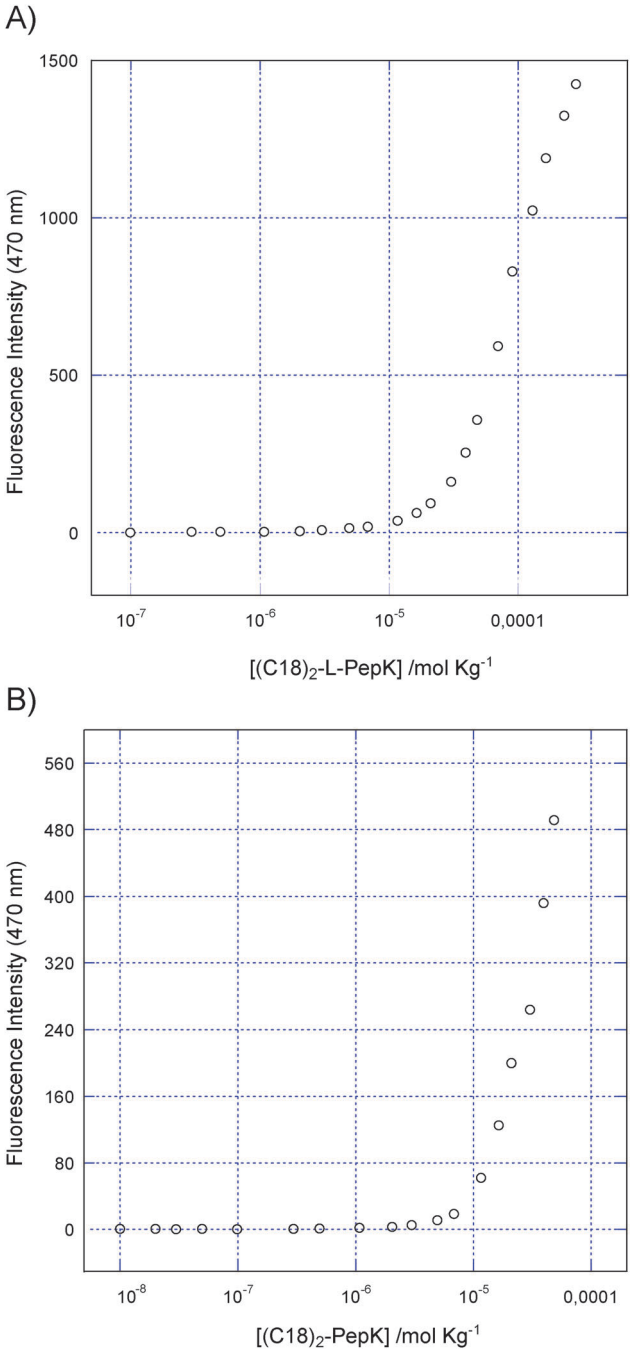

Fig. 2 Fluorescence intensity of the ANS fluorophore at 470 nm as a function of PAs [$(C18)_2$-L-PepK (A) and $(C18)_2$-PepK (B)] concentration; data are multiplied by a scale factor for a better comparison. CMC values are established from graphical break points.

translational diffusion coefficients in the Stokes–Einstein equation. An increase of the radius of 20% was observed for $(C18)_2$-PepE (100 nm) with respect to $(C18)_2$-PepK (80 nm) (see Fig. 3). Whereas only a slight difference in radii can be detected for the derivatives containing the spacer. Fluorescence measurements were carried out by exciting buffer solutions at 275 nm aiming to evaluate shifts of tyrosine fluorophore emission as a consequence of aromatic quenching on the surface of the aggregates. In Fig. 4 (upper panel)

Table 1 Structural parameters for the aggregates obtained from fluorescence measurements (critical micellar concentration values) and dynamic light scattering measurements (diffusion coefficients, D, hydrodynamic radii, R_H, and polydispersity indices)

Systems	CMC (mol kg^{-1})	R_H (nm)	$D \times 10^{-12}$ (m^2 s^{-1})	PDI
$(C18)_2$-PepK	7.0×10^{-6}	80 ± 27	3.1 ± 1.0	0.270
$(C18)_2$-L-PepK	1.9×10^{-5}	82 ± 34	3.1 ± 1.5	0.182
$(C18)_2$-PepE	3.9×10^{-5}	112 ± 44	1.9 ± 0.7	0.264
$(C18)_2$-L-PepE	3.2×10^{-5}	101 ± 39	2.4 ± 0.5	0.226

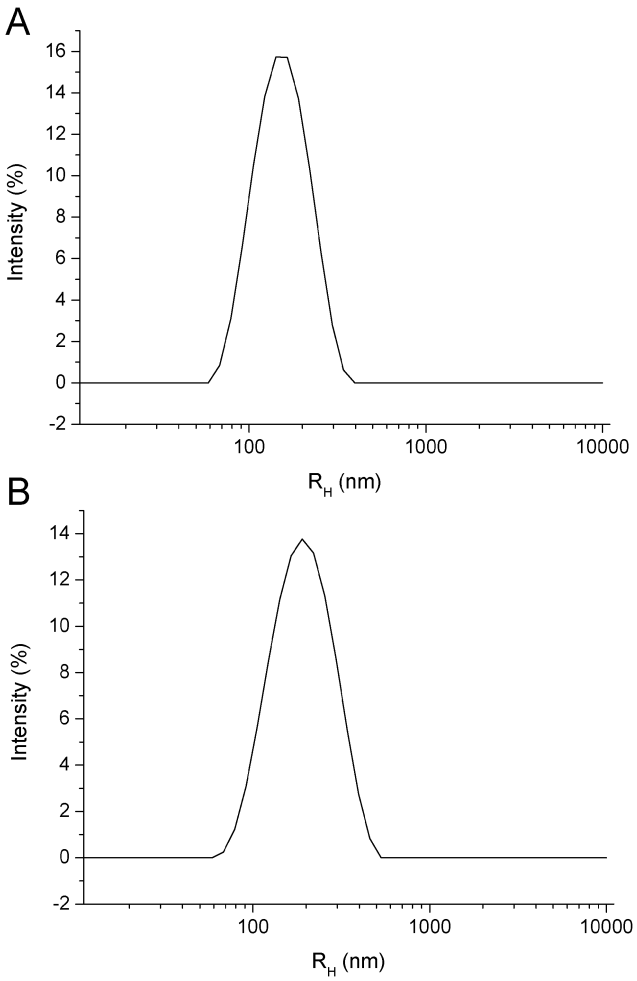

Fig. 3 DLS profiles of $(C18)_2$-PepK (A) and $(C18)_2$-PepE (B) peptide amphiphiles at a concentration of 2×10^{-4} M.

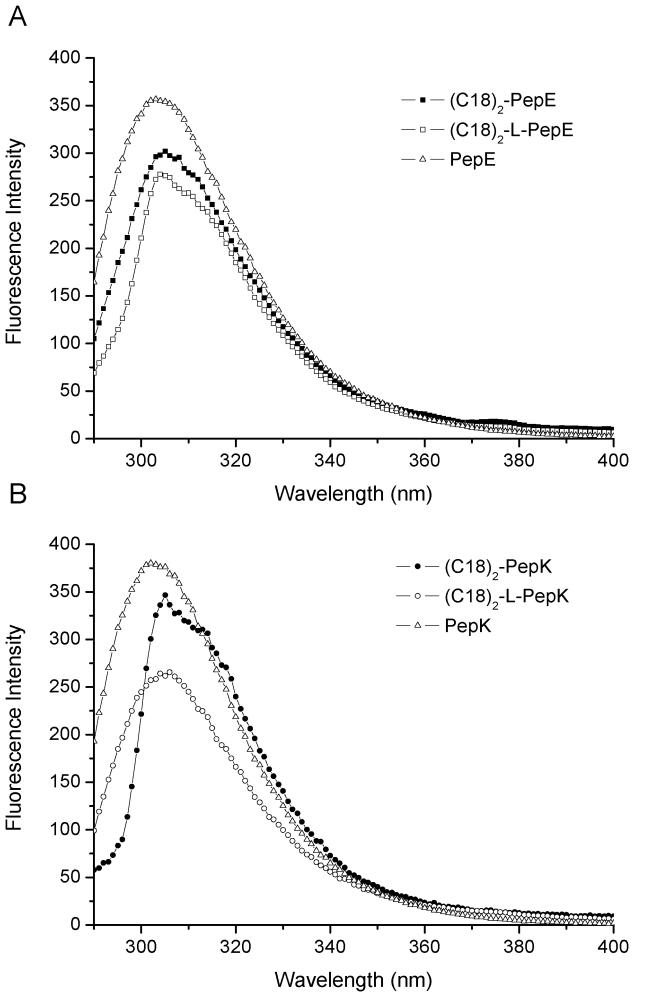

Fig. 4 Fluorescence emission spectra recorded by exciting buffer solutions at 275 nm for PepE derivatives (up) and PepK derivatives (down).

emission spectra for different PepE derivatives are reported. The behaviour of tyrosine does not show significant differences in intensity or in the wavelength shift. These results seem to exclude interaction among peptide side chains on the surfaces of aggregates. Similar results have been obtained for PepK derivatives (Fig. 4 lower panel).

3.3. Circular dichroism measurement

Conformational behaviours of PepE and PepK amphiphiles were investigated by CD spectroscopy. Lyophilized peptides were dissolved in the suitable weakly basic buffer (TRIS or PBS, see experimental section) at 2×10^{-4} M concentration. Under these experimental conditions, PAs are well above the CMC concentrations that have been determined by fluorescence and the presence of supramolecular aggregates in aqueous solution is fostered. In Fig. 5 the CD spectra of PepE (panel A) and PepK (panel B) derivatives are reported. The corresponding conformational preferences for all peptides were also analyzed by the CAPITO web-server.[30] The CD spectrum of $(C18)_2$-PepE does not show any propensity to fold as indicated by CD spectra, presenting a negative minimum at around 198 nm, typical for unordered structures. Moreover, the presence of the ethoxylic spacer does not influence significantly the dichroic bent of the PA. This trend was also confirmed by CAPITO analysis[30] (data not shown). Furthermore, two weak maxima at 208 and 232 nm are also detectable in the CD spectra of PepK derivatives (see Fig. 5B), in addition to the minimum at 196 nm. These spectra suggest that the replacement of the glutamic acid with the lysine at the C-terminus induces a rearrangement of the secondary structure with a partial folding of the IDP.

Further attempts to validate the CD results with more precise comparative conformational studies by NMR spectroscopy were

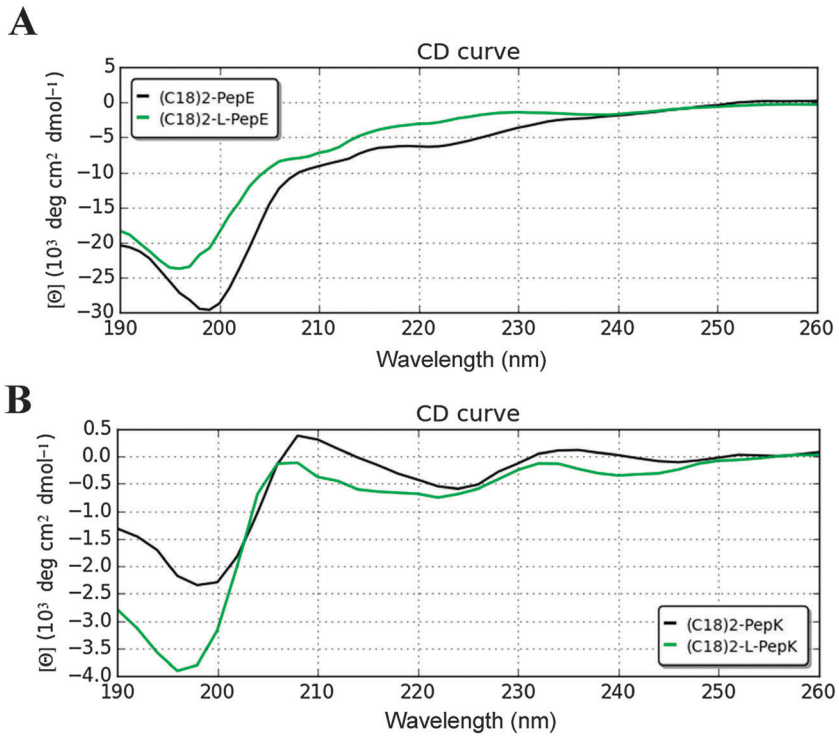

Fig. 5 CD spectra of: (A) $(C18)_2$-PepE and $(C18)_2$-L-PepE; and (B) $(C18)_2$-PepK and $(C18)_2$-L-PepK.

hampered by the high aggregation levels of PepE and PepK derivatives. Indeed, this aggregation produced sample precipitation and/or complete disappearance of signals in 1D [^{1}H] and 2D [^{1}H, ^{1}H] NMR spectra; this made impossible the process of resonance assignments.

3.4. Functional characterization: peptide effects on the CXCR4 receptor pathway

Then, the peptides $(C18)_2$-PepK, $(C18)_2$-L-PepK, $(C18)_2$-PepE, and $(C18)_2$-L-PepE, have been tested in order to determine:

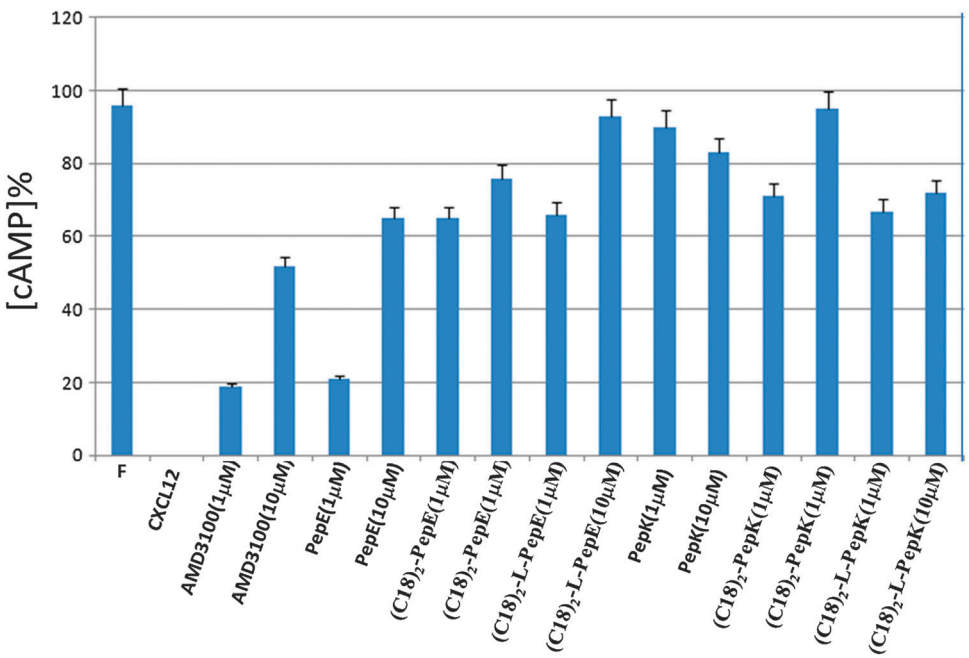

Fig. 6 Comparison of cAMP modulation by PepE, PepK, $(C18)_2$-PepE, $(C18)_2$-L-PepE, $(C18)_2$-PepK and $(C18)_2$-L-PepK and AMD3100 at 1 μM and 10 μM.

(i) peptide binding to the receptor through an indirect binding assay; (ii) the inhibition of CXCL12-induced migration; (iii) cAMP levels. The results were compared to the ones for AMD3100 that is the lead CXCR4 antagonist.[26] The binding of the four peptides to CXCR4 was evaluated in CCRF-CEM using a CXCR4 12G5 monoclonal antibody as previously described,[31] and two concentrations (1 μM and 10 μM) which are matching the ones previously used in CXCR4 binding assays.

The four peptides did not displace 12G5 antibody compared to AMD3100, which strongly reduced antibody binding to CXCR4. These behaviours agree with those previously obtained for the free PepE and PepK peptides.[14] This could be explained considering the different binding sites on AMD3100/12G5 antibody and the four highly flexible and disordered peptides. Also, a migration assay was performed and the four peptides resulted to reduce the migration of CCRF-CEM cells towards CXCL12 even if they showed less activity than AMD3100 (data not shown).

Taking into account that CXCR4 is a G-Protein coupled receptor, it inhibits through the G-protein the adenylate cyclase activity and fosters the cAMP production as ''second messenger''.[25] As a result of the binding to CXCL12, we also evaluated the cAMP levels after treatment with the four peptides. The results indicate that in the presence of CXCL12 (100 ng mL^{-1}) and Forskolin (1 μM): (i) $(C18)_2$-PepK, $(C18)_2$-L-PepK, $(C18)_2$-PepE, and $(C18)_2$-L-PepE show a dose dependent increase of the cAMP level of about 66% at the lower dose (1 μM) and of 84% at the higher dose (10 μM); (ii) at 10 μM, $(C18)_2$-L-PepK increases cAMP levels up to 93% and $(C18)_2$-PepE increases the cAMP level to 95%; (iii) AMD3100 exhibits less efficient activities on the adenylate cyclase when compared to the four peptides (Fig. 6).

4. Conclusions

We have explored the possibility that intrinsically disordered peptides could be used as polar heads connected to alkyl chains to generate new molecular buildings for drug delivery vehicles in cells over-expressing the CXCR4 receptor. In our previous investigations, two peptides were synthesized and studied by NMR and CD spectroscopy.[32] These compounds were indicated as PepE and PepK due to the presence of a glutamic acid or a lysine residue at the C-terminus. The absence of regular secondary structure elements confirmed the natively disordered nature of these peptides.

In the present study, we have investigated the opportunity to induce conformational rearrangement by modifying these peptide sequences with two alkyl chains of eighteen carbon atoms each and with an ethoxylic linker. In fact, the insertion on peptides of aliphatic moieties pushes the resulting amphiphilic molecules to self-assemble in supramolecular aggregates. Once confined on the external surface of the aggregates, peptides could undergo a disorder-to-order transition.[32] As demonstrated by fluorescence and DLS studies, all the designed PAs are able to self-assemble in large aggregates with an average diameter ranging between 80 and 110 nm, independently from their charge and from the presence of the PEG spacer.

All four PAs are strongly aggregated and poorly soluble at high concentrations (0.50–1.0 mM). These characteristics made them unsuitable for characterization performed by means of solution NMR techniques; even after changing the experimental conditions such as implementing buffers at different pH and temperatures.

CMC values comply with those previously found for peptide amphiphiles containing the same hydrophobic moiety and they point out the high stability of the aggregates.[28,29] The higher CMC values of $(C18)_2$-PepE and $(C18)_2$-L-PepE indicate a lower propensity to aggregate if compared with the corresponding PepK derivatives. Also after the insertion of the hydrophobic portion, PepE keeps its tendency towards the disordered/unfolded state from the conformational point of view. Whereas both the PepK derivatives show a partial folding, with respect to the free peptide sequence. To the best of our knowledge, these compounds are the first CPC motif containing amphiphilic peptides which are able to aggregate. Comparing the four peptide derivatives with previously studied PepE and PepK sequences[14], we can point out that (i) all peptides did not show an evident binding affinity for CXCR4; (ii) the best result about the migration assay was obtained for PepE sequences; and (iii) the highest cAMP percentages were obtained for $(C18)_2$-L-PepE- (93%) and $(C18)_2$-L-PepK (95%) at 10 μM (Fig. 6).

According to these preliminary results, these PA systems could be further modified to realize new supramolecular peptide-based compounds, able to be encapsulated by living cells for biomedical industrial application.

Abbreviations

AhOh	21-Amino-4,7,10,13,16,19-hexaoxaheneicosanoic acid
ANS	8-Anilino-1-naphthalene sulfonic acid ammonium salt
CMC	Critical micellar concentration
cAMP	Cyclic adenosine monophosphate
CD	Circular dichroism
DCM	Dichloromethane
DIEA	*N*,*N*-Diisopropylethylamine
DLS	Dynamic light scattering
DMF	*N*,*N*-Dimethylformamide
DPC	*n*-Dodecyl phosphatidylcholine
EDTA	Ethylenediaminetetraacetic acid
Fmoc	9-Fluorenylmethoxycarbonyl
G-CSF	Granulocyte-colony stimulating factor
GTP	Guanine nucleotide triphosphate
HBTU	O-benzotriazole-tetramethyl-uronium-hexafluoro-phosphate
IDP	Intrinsically disordered protein or peptide
MD	Molecular dynamics
PAs	Peptide amphiphiles
PBS	Phosphate buffer
RP-HPLC	Reverse-phase high-pressure liquid chromatography
SPPS	Solid phase peptide synthesis

TFA	Trifluoroacetic acid
TIS	Triisopropylsilane
TRIS buffer	Tris(hydroxymethyl)aminomethane

Acknowledgements

Marian Vincenzi thanks the Università Italo Francese (UIF) for financial support, project C2-1, 2014/38723, cap. 6.01.1810 UIF. Luisa Ronga and Jean Guillon thank the ''Plateforme Protéome'' of the University of Bordeaux for the access to the Ultraflex III TOF/TOF mass spectrometer and the valuable advice regarding its use.

References

1 G. Wider, K. H. Lee and K. Wuthrich, *J. Mol. Biol.*, 1982, **155**, 367–388.
2 L. Zetta, P. J. Hore and R. Kaptein, *Eur. J. Biochem.*, 1983, **134**, 371–376.
3 F. Naider, L. A. Jelicks, J. M. Becker and M. S. Broido, *Biopolymers*, 1989, **28**, 487–497.
4 L. R. Brown, W. Braun, A. Kumar and K. Wuthrich, *Biophys. J.*, 1982, **37**, 319.
5 J. K. Lakey, D. Baty and F. Pattus, *J. Mol. Biol.*, 1991, **218**, 639–653.
6 A. A. Kaspar and J. M. Reichert, *Drug Discovery Today*, 2013, **18**(17/18), 807–817.
7 K. Fosgerau and T. Hoffmann, *Drug Discovery Today*, 2015, **20**(1), 122–128.
8 E. Benedetti, L. Aloj, G. Morelli, A. Accardo, R. Mansi and D. Tesauro, *BioDrugs*, 2004, **18**, 279–295.
9 M. F. Tweedle, *Acc. Chem. Res.*, 2009, **42**(7), 958–968.
10 V. J. Hruby and M. Cai, *Annu. Rev. Pharmacol. Toxicol.*, 2013, **53**, 557–580.
11 J. C. Reubi, *Endocr. Rev.*, 2003, **24**(4), 389–427.
12 W. T. Choi, S. Duggineni, Y. Xu and Z. Huang, *J. Med. Chem.*, 2012, **55**, 977–994.
13 S. Costantini, R. Raucci, G. Colonna, F. A. Mercurio, A. M. Trotta, P. Ringhieri, M. Leone, F. Rossi, C. Pellegrino, G. Castello and S. Scala, *J. Pept. Sci.*, 2014, **20**, 270–278.
14 M. Vincenzi, S. Costantini, S. Scala, D. Tesauro, A. Accardo, M. Leone, G. Colonna, J. Guillon, L. Portella, A. M. Trotta, L. Ronga and F. Rossi, *Int. J. Mol. Sci.*, 2015, **16**, 12159–12173.
15 S. Banta, Z. Megeed, M. Casali, K. Regeand and M. L. Yarmush, *J. Nanosci. Nanotechnol.*, 2007, **7**, 387–401.
16 I. W. Hamley, *Soft Matter*, 2011, **7**, 4122–4138.
17 F. Versluis, H. R. Marsden and A. Kros, *Chem. Soc. Rev.*, 2010, **39**, 3434–3444.
18 T. R. Pearce, K. Shroff and E. Kokkoli, *Adv. Mater.*, 2012, **24**, 3803–3822.
19 A. Accardo, G. Salsano, A. Morisco, M. Aurilio, A. Parisi, F. Maione, C. Cicala, D. Tesauro, L. Aloj, G. De Rosa and G. Morelli, *Int. J. Nanomed.*, 2012, **7**, 2007–2017.
20 Y. Zhang, H. Zhang, X. Wang, J. Wang, X. Zhang and Q. Zhang, *Biomaterials*, 2012, **33**, 679–691.
21 A. Accardo, L. Aloj, M. Aurilio, G. Morelli and D. Tesauro, *Int. J. Nanomed.*, 2014, **9**, 1537–1557.
22 L. Schmitt and C. Dietrich, *J. Am. Chem. Soc.*, 1994, **116**, 8485–8491.
23 A. Accardo, R. Mansi, A. Morisco, G. Mangiapia, L. Paduano, D. Tesauro, A. Radulescu, M. Aurilio, L. Aloj, C. Arra and G. Morelli, *Mol. BioSyst.*, 2010, **6**, 878–887.
24 A. Accardo, D. Tesauro, G. Mangiapia, C. Pedone and G. Morelli, *Pept. Sci. Biopolym.*, 2007, **88**, 115–121.
25 E. De Clercq, *Biochem. Pharmacol.*, 2009, **77**, 1655–1664.
26 L. Portella, R. Vitale, S. De Luca, C. D'Alterio, C. Ieranò, M. Napolitano, A. Riccio, M. N. Polimeno, L. Monfregola, A. Barbieri, A. Luciano, A. Ciarmiello, C. Arra, G. Castello, P. Amodeo and S. Scala, *PLoS One*, 2013, **8**(9), e74548.
27 Y. Matsumura and H. Maeda, *Cancer Res.*, 1986, **46**, 6387–6392.
28 A. Accardo, A. Morisco, P. Palladino, R. Palumbo, D. Tesauro and G. Morelli, *Mol. BioSyst.*, 2011, **7**, 862–870.
29 A. Morisco, A. Accardo, E. Gianolio, E. Gianolio, D. Tesauro, E. Bendetti, G. Morelli, D. Tesauro, E. Bendetti and G. Morelli, *J. Pept. Sci.*, 2009, **15**, 242–250.
30 C. I. Wiedemann, P. Bellstedt and M. Görlach, *Bioinformatics*, 2013, **29**, 1750–1757.
31 B. A. Teicher and S. P. Fricker, *Clin. Cancer Res.*, 2010, **16**, 2927–2931.
32 A. Accardo, M. Leone, D. Tesauro, R. Aufiero, A. Bénarouche, J.-F. Cavalier, S. Longhi, F. Carriere and F. Rossi, *Mol. BioSyst.*, 2013, **9**, 1401–1410.

